NUMERICAL MODELLING OF REVERSE PULSE CLEANING ON RIGID CERAMIC FILTERS

T. G. Chuah[1], J. P. K. Seville[2] and C. J. Withers[3]

[1]*Department of Chemical and Environmental Engineering, Faculty of Engineering, Universiti Putra Malaysia, 43400 UPM, Serdang, Selangor.*

[2]*School of Chemical Engineering, The University of Birmingham, Edgbaston, Birmingham B15 2TT, UK*

[3]*Caldo Environmental Engineering Ltd, 1 Shire Business Park, Wainwright Road, Worcester, WR4 9FA, UK*

ABSTRACT

Many industrial processes involve the generation of waste gases and particulates. Environmental legislation enacted as a result of government policy has compelled industry to pay a serious attention to the air pollution issue. It has driven to the need to install air pollution control equipment. Rigid ceramic filters have proved themselves as highly efficient gas filtration devices in particles emission control. However, the filter cleaning mechanisms are still not fully understood. A computer program is developed to model the flow of the reverse pulse air from the cleaning bar nozzle to the dusty side of the filter. The program uses an iterative calculation mode of Microsoft Excel and allows variables such as reverse pulse pressure and filter geometry to be changed. Predictions are carried out on various pulse tube distances, temperatures of gas flow and various friction factors in order to study their effects on pressure distribution. The simulation is validated by data obtained from previous experiment works and fair agreement is achieved.

Keywords : *Gas Filtration, Ceramic Filter, Pulse Cleaning, Modelling, Flow Dynamics*

1.0 Introduction

Malaysia possesses a great potential market for hot gas cleaning technology. The country has made great strides in economic development during the last two decades. It is endowed with rich natural resources, such as oil and gas which provide the nation's energy requirements and a feedstock for the development of manufacturing and industry. Although Malaysia can be considered as one of the least polluted urban environments in Asia, rapid urbanisation and sustained economic growth together with the high demand for transportation have contributed towards air pollution issues. With the shift in the nation's strategy from that of agriculture towards manufacturing and heavy industries, a rapid increase in the generation of pollutants and wastes, which will result in the deterioration of air and water quality can be foreseen. The goal of the country to achieve industrial country status by the year 2020 and the associated industrial and urban expansion will further strain the environment in Malaysia. The problem of air pollution is particularly critical in urban industrial areas like Klang Valley. The deteriorating state of air quality in this area has been due to the presence of suspended particulates or dust generated by disposal of industrial, municipal and agricultural waste through open burning. Apart from these, the problem is also worsened by the emission from the power generation plants and by industrial combustion.

Rigid ceramic filters represent the most promising technology for particulate removal from process gases at high temperature [1]. Ceramic filters are normally used in the form of "candles": cylindrical tubes with permeable walls. Two generic types are available, with granular and fibrous structures. Effective cleaning of the filter element is as important as the filtration process and it is important to study the gas flow dynamics in the reverse flow mode in order to achieve better filter cleaning. Several studies have been carried out on pulse gas cleaning [2, 3, 4, 5]. All these studies have shown that the reverse pulse pressure is not usually uniformly distributed along the filter element. It is generally agreed that the pressure is greatest at the closed end of the candle and at a minimum, or even close to zero, at the open end.

In this paper, a new simulation method for predicting the flow field during the filter cleaning process is proposed. A computer program has been written to model the flow of the reverse pulse air, from the cleaning bar nozzle to the dirty side of the filter. The program uses an iterative calculation mode and allows variables such as pulse pressure and filter geometry to be changed. The model has been used to investigate the effect of the operational parameters and filter properties such as pulse tube distance, friction factor, pulse gas temperature, reverse pulse pressure and reverse flow rate on the pressure difference over the candle wall and axial velocity profile. The results are compared with the experimental data obtained from Mai *et al.* [6] and Stephen *et al.* [7].

2.0 Description of the Model

The simulation program includes calculation of the contributions of the nozzle jet and the entrained flow at the filter inlet; it then computes the gas volume flow rate through the orifice and along the filter element.

Figure 1 shows the flow maldistribution in a filter during filtration operation. Airflow from the cleaning bar is a function of reservoir pressure and hole diameter. The jet entrains more gas as it fans out towards the top of the filter element. At the

top of the element the gas mixture has an axial velocity which is a function of the airflow from the cleaning bar and the distance between the leaning bar and the filter element.

At the very bottom of the filter element the axial velocity is zero. The internal pressure at this point is equal to the velocity head at the top of the element minus the friction loss between the two points. This internal pressure causes the gas to flow radially out through the filter wall. The gas flow rate is a function of the permeability of the filter medium and the internal pressure.

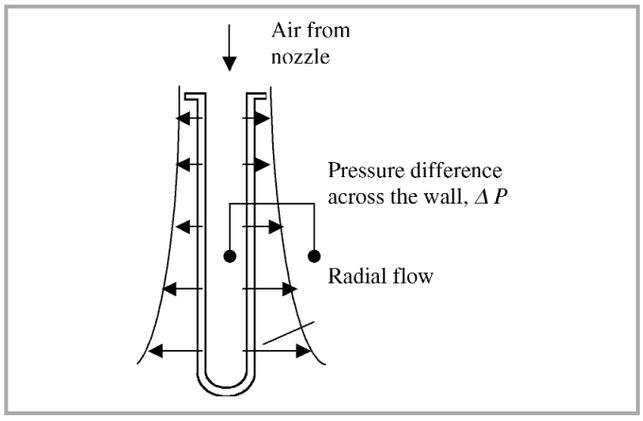

Figure 1: Flow maldistribution along filter during reverse pulse

The pressure drop across the wall is related to the resistance to flow of the filter medium and can be calculated using Darcy's Law for flow through a porous medium (in the appropriate form for a thick wall cylinder):

$$\Delta P = K\mu U\left[\ln\left(\frac{D_o}{Di}\right)\left(\frac{D_o}{2}\right)\right] \qquad (1)$$

Where K is resistance of the filter medium, μ is the gas viscosity, D_o and D_i indicate the external and internal diameters of filter.

Just above the bottom of the filter, the axial velocity is greater than zero and the internal pressure is slightly less than at the very bottom. The internal pressure generates further radial flow, resulting in greater axial flow and a decrease in internal pressure at the next position up through to the top of element. The total radial flow is a function of the inlet velocity and medium permeability. Total radial flow cannot exceed the gas inlet flow. The mathematical description of this model is shown as follow.

a) Nozzle position and discharge rate

The optimum distance between the gas discharge orifice and the filter inlet, and the resulting gas flow rate through the orifice, are calculated based on basic fluid mechanics.

i) Distance from the nozzle to the filter element at optimum jet angle and perfect positioning (see Figure 2):

$$x = \frac{D_{or}}{2}\tan[((\alpha/2)/(360/2\pi))]^{1} \qquad (2)$$

where jet angle, $\alpha = 20^{o}$ for $\frac{x}{D_{or}} < 100$

ii) Gas volumetric flow rate for sonic flow through orifice of cross-section area, A_o:

$$q = \frac{C_1 C A_{or}\rho_g}{\sqrt{T_g}} = \pi\frac{D_{or}^2 C_1 C\rho_g}{4\sqrt{T_g}} \qquad (3)$$

where C, C_1 are dimensionless constants and T_g is the absolute temperature of the gas stream.

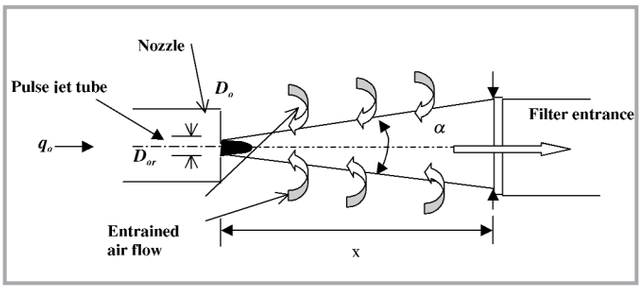

Figure 2: Schematic diagram of pulse gas flow for pulse jet tube and filter element

b) Filter inlet

The entrance flow rate and the gas velocity entering the element are calculated.

iii) Total gas flow Q_{total} at the entrance of the filter element:

$$Q_{total} = q_o(0.32)\frac{x}{D_o} \qquad \text{for } 7 < \frac{x}{D_o} < 100 \qquad (4)$$

where x is the distance from the nozzle to the filter entrance.

iv) Velocity at the entrance of the filter element:

$$U = \frac{Q}{A_f} \qquad (5)$$

where A_f is the cross-sectional area at entrance of the filter.

v) Velocity head, static head equivalent of the kinetic energy in the stream of uniform velocity U_f (from Bernoulli's equation):

$$P_h = \frac{1}{2}U_f^{2}\rho_g \qquad (6)$$

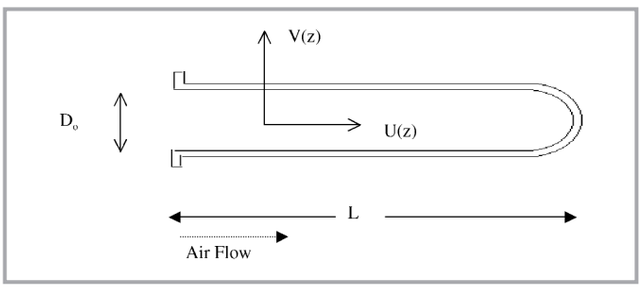

Figure 3: Schematic diagram of axial and radial directions flows in a filter

c) Filter tube

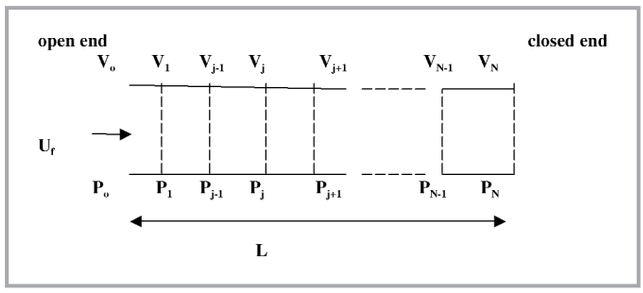

Figure 4: Description of flow in the filter element

The length of the filter L is divided into equally spaced nodes, N. Starting from Eq. (7) to Eq. (13), pressure distribution is estimated by iterative calculations of the parameters *V, U* and *P* along the filter element, taking into account element geometry and resistance. Boundary conditions, are (a) filtration pressure is provided at the inlet of the filter and (b) at the end of the filter, the volume flow rate is set to zero, i.e. no gas flow is permitted through the close end.

vi) Axial gas flow area, A_f:

$$A_{f,j} = \pi \frac{D_j^{\,2}}{4} \tag{7}$$

where D_j denotes the internal diameter of the filter at the position of the j-th node.

vii) Cylindrical surface area of radial gas flow at j-th node, A_R:

$$A_{R,j} = \pi l D_j \frac{L}{N-1} \tag{8}$$

viii) Gas differential volume flow rate through filter element wall, V:

$$V_j = \left[\frac{A_{R,j} \Delta P_j}{K} \right] \tag{9}$$

where subscript j denotes the variables are evaluated at node-j.

ix) Cumulative loss of gas flow rate through the filter element walls preceding node-j:

$$F_j = \sum_1^j V_j \tag{10}$$

since there is no flux through the end of the filter at $z=L$, $Q = \sum_1^N V_j$

x) Axial superficial gas velocity at j-th position

$$U_j = U - \frac{F_j}{A_{f,j}} \tag{11}$$

xi) Static equivalent velocity head at j-th position:

$$P_{h,j} = U_j^{\,2} \rho \tag{12}$$

xii) Static equivalent pressure head at j-th position

$$P_j = P_{hj} \tag{13}$$

3.0 Effect of Pulse Tube Distance

The model is used to investigate the effect of the pulse tube position, relative to the open-end of the filter candle, on the pressure difference along the filter element. Grannell [8] previously studied the optimisation of the pulse tube placement by experiments. Using this model, comparison with his data was carried out. For the purpose of this study, the Eq. (2) was neglected and a fixed value of the pulse tube distance, ***x***, was used in Eq. (4) for calculation of the total gas flow, Q_{total}, at the entrance to the filter element. Figure 5 shows the schematic diagram of the distance of the pulse tube position. ***x*** indicates the distance of pulse jet tube from the open end of the filter.

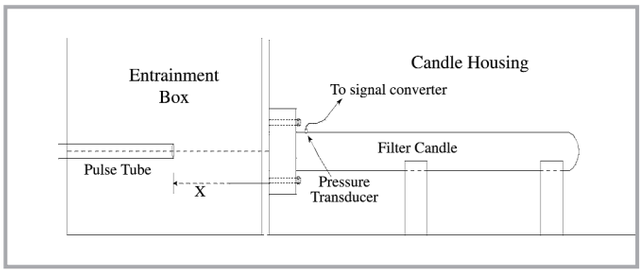

***Figure 5: Schematic diagram showing measurement of pulse tube distance* [8]**

Grannell [8] found that 13.5cm from the open end was the optimum distance for a 40 mm candle opening as this was the distance at which no "secondary" entrainment of gas occurred through the filter wall (for 4 bar cleaning pulse pressure).

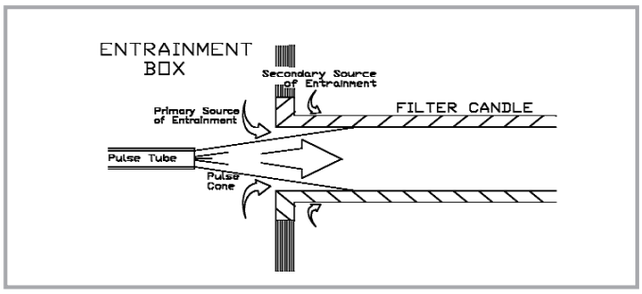

Figure 6: Pulse tube distance too short

Secondary entrainment is normally caused by the pulse tube being too close to the filter opening. As the gas was pulsed from the tube a large quantity of pulse gas extends into the filter. Secondary entrainment gas enters from the throat of the filter (Figure 6) in the opposite direction to the cleaning flow and will suck dusty gas through the round of throat of the filter. After several cycles of conditioning, dust cake will be retained around the open end of the filter and is difficult to detach [7].

Figure 7 shows the comparison between the simulation and the data obtained from Grannell's experiments. In his work, the

range of pulse tube distance over which the secondary entrainment occurred was between 8 and 14 cm.

Two pulse tube distances are used in this simulation, 12 and 13.5cm (optimum distance according to Grannell [8]). The simulation gave a good agreement with the experimental data. The model henceforth will be used to predict the effect of the tube distance on the pressure difference profile.

Figure 8 shows the effect of two different pulse tube distances, 8cm and 15cm, on the pressure difference profile. As the tube distance increases from 8cm to 12cm, the peak pressure at the closed end of the candle increased by 150%.

For a pulse tube distance of 15cm, the peak pressure increases by about 180% compared with the pressure at a pulse tube distance of 8cm. This increment in the pressure difference was due to a larger quantity of gas being forced into the filter flow at the greater tube distance. Larger axial velocities were converted into gas momentum and hence contributed to the pressure difference across the filter wall. However, as the distance increased, the rise of the pressure difference became less significant.

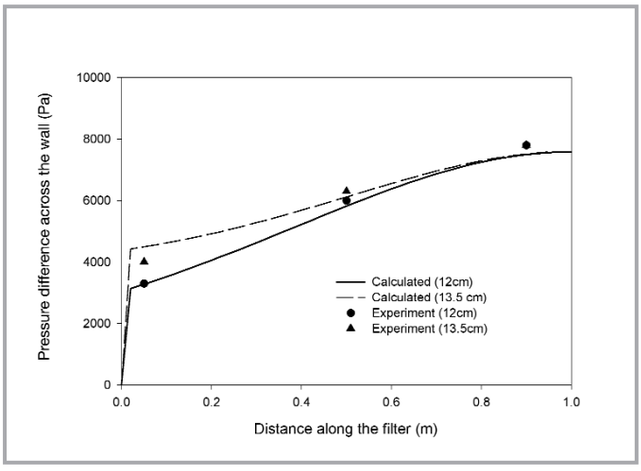

Figure 7:Comparison of the simulation and the experimental data with a pulse pressure of 4 bar

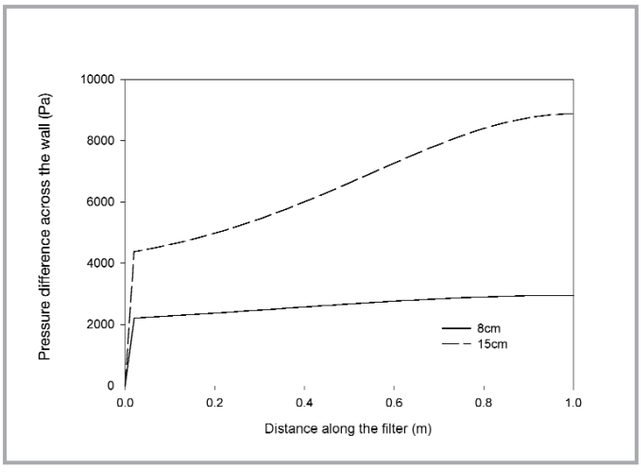

Figure 8:Effect of the pulse tube distance from the open end to the pressure difference with a pulse pressure of 4 bar

4.0 Effect of Friction Factor

Figure 9 shows the variation in the local pressure difference across the filter wall from the open end to the closed end using three different friction factors, 0.01, 0.05 and 0.1 respectively (corresponding to a surface roughness of 1mm, 6.5mm and 15mm respectively, calculated by Colebrook-White equation [9]. For the flow in the filter with a friction factor of 0.01, it can be seen that local pressure difference across the wall increases from the open end to the closed end. A different outcome was noticed for the case when the internal wall friction was 0.05; the local pressure difference across the wall now decreased with increasing distance from the open end of the filter. Increasing friction factor will hence reduce the pressure drop as described in Eq. (14).

$$\frac{dP}{dz}+\frac{1}{2}\frac{d}{dz}(\rho u_z^{\,2})=-4\frac{f}{D_i}\frac{1}{2}\rho u_z^{\,2} \qquad (14)$$

However, the profile of the decrement of the pressure difference was not continuous; it passes through a minimum before the closed end was reached. The effect of the friction was also noticed when the friction factor was increased to 0.1.

There was an initial decrease in the pressure difference across the wall at the open end; this reached a minimum at a distance 70cm from the open end. There was a slight increment in the pressure difference across the filter wall close to the closed end.

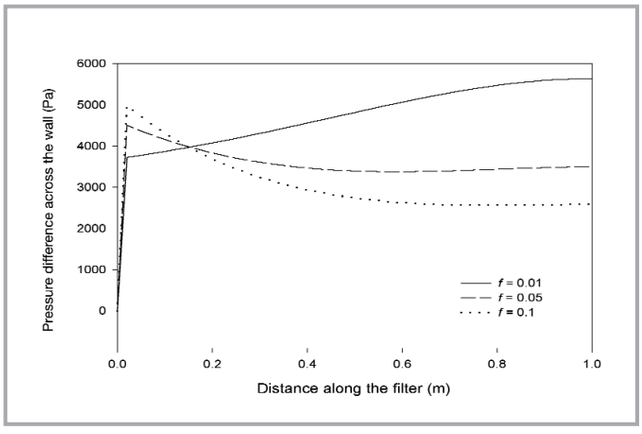

Figure 9: Effect of the friction factor on the pressure difference profile with a reverse pulse pressure 4 bar

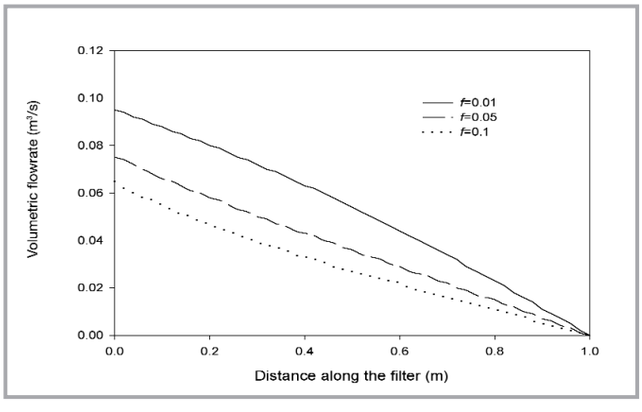

Figure 10: Effect of the friction factor on the pressure difference profile with a reverse pulse pressure of 4 bar

Figure 10 shows the changes of volumetric flowrate along the filter candle for different friction factors. At higher friction factor, greater volumetric flow rate decreased from the open end of the filter towards the closed end of the filter. As the gas flow travelled along the filter from the open end to the closed end of the filter, the axial velocity was recovered as static head, thus increasing the pressure difference across the wall. The volumetric flow rate was decreased monotonically to reach zero at the closed end. For friction factors of 0.05 and 0.1, with a large volumetric flowrate at the open end, the frictional effects are large and the pressure difference across the wall was decreased. However, at a distance of 60cm from the open end, the pressure drop caused by friction is reduced because the volumetric flow is then small and makes little contribution to the pressure difference across the wall. The loss of momentum of gas flow then dominates the axial pressure drop and pressure recovery occurs. The frictional pressure drop scales with Q^2. Hence, as Q decreases, the contribution of the frictional terms reduces strongly.

5.0 Effect of Temperatures

An important concern in filter cleaning is the progressive loss in filter strength with use. The thermal stress set up during pulse cleaning will weaken the ceramic substrate of the filters. For the cleaning process, a high temperature jet of gas can be reverse pulsed through the hot ceramic filter, this should be at a temperature greater than ambient. This is to avoid the thermal stresses set up during pulse cleaning which will weaken the ceramic substrate. Research at University of Aachen [10] has confirmed that a severe temperature transient occurs during pulse cleaning when using `cold' pulse gas. To reduce this problem, Biffin *et al.* [11] has carried the experiments by re-entrained filtered hot gas to use for filter pulse cleaning by introducing a venturi educer.

Figure 11 shows the effect of the pulse jet gas temperature on the pressure difference profile along the filter element. When the temperature of the jet gas was increased, from 20ºC to 200ºoC, the pressure difference increased by 23% at the open end and 15% at the closed end of the filter. However, at the higher temperatures, 300ºC and 400ºC, the open end pressure differences were 32% and 38% respectively higher than at 20ºC, with very little increment in the pressure difference at the closed end.

At 20ºC, the local pressure increased with increasing distance from the open end of the filter candle, but the change of local pressure was reduced at higher temperatures and was not significant. At a temperature of 20ºC, the pressure difference increased 63% from the open end to the closed end, whist at 300ºC and 400ºC the pressure difference at the closed end was only 35% and 30% higher from the open end respectively.

Increasing temperature will increase the gas viscosity and hence will increase the pressure drop across the filter wall. But at the same time the gas density will decrease with increasing temperature and hence reduce the pressure changes along the filter candle, which are largely due to momentum effects. The combination of these effects tends to reduce non-uniformity, as shown in Figure 11.

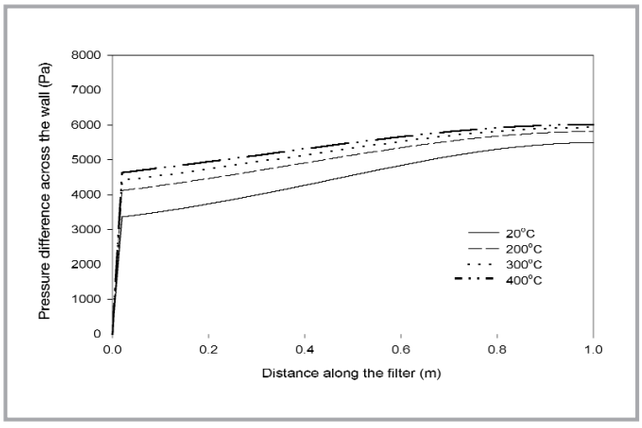

Figure 11: Effect of pulse jet temperatures on pressure difference profile

6.0 Comparison with Previous Work

In order to assess the accuracy of the model, the results were compared with experimental data obtained from previous studies [6, 7].

6.1 Comparison with the DIA-Schumalith F40 Filter Candle [6]

The pressure distribution in the candle elements is shown in Figure 12 in which the pulse cleaning pressure was 5 bar. Inside the filter candle, continuous outflow in a radial direction reduces the axial velocity. Kinetic energy is then converted into pressure energy, so that the pressure increases approaching the closed end of the candle. The simulation shows good agreement with the measurements for the positions 15 and 50cm, but overestimated the pressure at the closed end, presumably because not all the kinetic energy was recovered as pressure.

One factor here is that the Excel simulation neglects pressure loss due to frictional effects. Inadequate fitting of the model near the closed end could also be the result of the influence of the unequal distribution of porosity and resistance along the filter candle elements. Strong local pressure fluctuations during the measurements can also lead to errors, usually reducing the accuracy of the measured pressure difference. Only 3 measurement points were used in these studies; more data should be provided in order to get a better comparison.

6.2 Comparison with Cerafil-S Filter Candles [7]

Figures 13 shows the pressure profiles along the filter elements with pulse cleaning pressures of 4 bar at an initial (pre cleaning) filtration pressure difference of 550 Pa. The pressure difference predicted from the simulation was lower than the experimental data obtained from Stephen *et al.* [7]. The difference could be because of the experimental set up, *e.g.* the distance of the pulse tube from the open end of the filter and the filter resistance may be different from the current simulation.

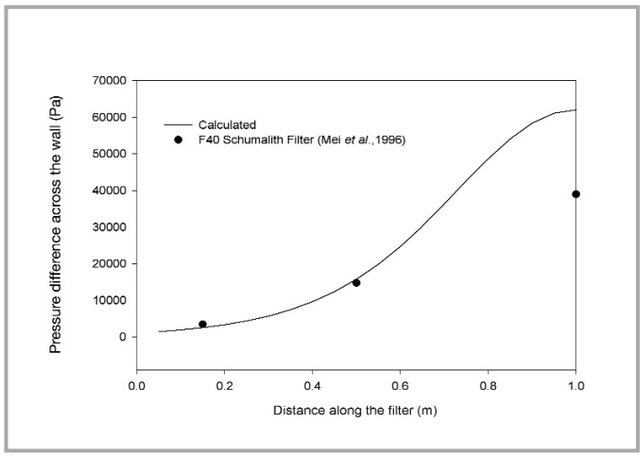

Figure 12: Distribution of cleaning pressure in a DIA-Schumalith F40 filter

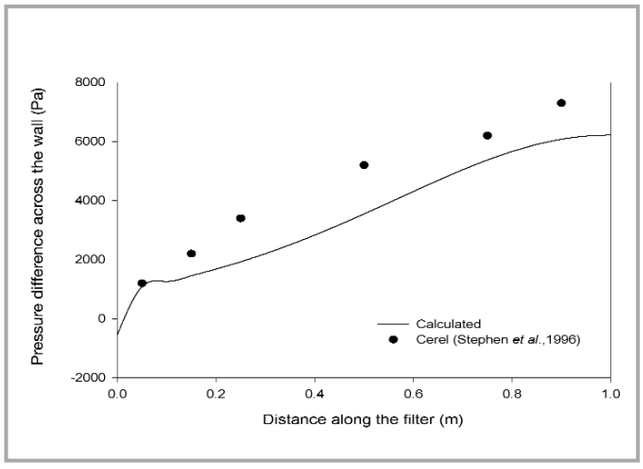

Figure 13: Pressure distribution on a Cerafil filter candle with a 4 bar pulse pressure (filtration pressure 550Pa)

7.0 Conclusions

The mathematical model seems able to predict the pressure drop and velocity profile along a filter element during reverse flow cleaning. Simulations showed the distance of the pulse tube had an effect on the cleaning pressure distribution. A large pulse tube distance will increase the pressure difference in the filter due to the larger volumetric gas flow that has been converted into gas momentum and contributes to the pressure difference across the filter wall. At larger distances, the increment of the pressure difference became less significant.

The simulation also showed that at higher friction factors, the pressure difference across the filter wall did not decrease continuously; it passed through a minimum before the closed end was reached. For higher friction factors, with a large volumetric flowrate at the open end, the friction dominated and the pressure difference across the wall was decreased.

Increasing temperature increases the gas viscosity, thus, the pressure drop across the filter also increased. However, the gas density decreased with increasing temperature, hence reducing the pressure changes along the filter candle. The combination of effects makes the pressure difference across the wall more uniform. ■

Nomenclatures

A_l : Axial gas flow area (m^2)
A_{or} : Cross section area of nozzle (m^2)
A_R : Cylindrical surface area of radial gas flow (m^2)
C : Coefficient of discharge, normally taken as 0.99
C_l : Dimensional constant, 0.0405 (SI units)
D_i : Filter internal diameter (m)
D_o : Filter external diameter (m)
D_{or} : Nozzle diameter (m)
F : Cumulative flow rate through filter element (m^3)
K : Resistance to flow (m^{-1})
L : Length of filter element (m)
P : Pressure (Pa)
P_h : Velocity head (Pa)
P_o : Ambient pressure from surrounding filter element (Pa)
ΔP : Pressure difference (Pa)
Q_{total} : Total gas volumetric flow rate into the filter (m^3s^{-1})
q_o : Gas volumetric flow rate through nozzle (kgs^{-1})
T_g : Absolute gas temperature, (K)
U : Gas velocity (ms^{-1})
V : Gas volume flow rate (m^3s^{-1})
x : Distance from orifice to filter element (m)
z : Position along the candle
ρ : Gas density (kgm^{-3})
α : Jet gas angle, ^{o}

Subscripts

f : filter element
g : gas (air)
j : position along filter element
N : position along filter element

REFERENCES

1. Seville J. P. K. (1997). "Rigid Ceramic Filters" in "Gas Cleaning in Demanding Applications". Seville, J. P. K. (editor), Blackie Academic and Professional, Glasgow, pp. 96-129.
2. Berbner, S., Löffler, F.(1993). "Pulse Cleaning of Rigid Ceramic Filter Elements at High Temperatures" in "Gas Cleaning at High Temperature" R.Clift and J.P.K. Seville (Eds.), Blackie Academic & Professional, Glasgow, pp. 225-243.
3. Laux, S., Giernoth, B., Bulak, H., Renz, U. (1993). "Aspects of Pulse-Jet Cleaning of Ceramic Filter Elements" in "Gas Cleaning at High Temperatures" R.Clift and J.P.K. Seville (Eds.), Blackie Academic & Professional, Glasgow, pp.203-224.
4. Ito, S. (1993). "Pulse Jet Cleaning and Internal Flow in a Large Ceramic Tube Filter", in "Gas Cleaning at High Temperatures", R.Clift and J.P.K. Seville (Eds.), Blackie Academic & Professional, Glasgow, pp. 266-279.
5. Chuah, T. G., Withers, C. J., Burbidge, A. S., Seville, J. P. K.(1999). "Numerical Modelling of Reverse Pulse Cleaning" in "High Temperature Gas Cleaning", A. Dittler, G. Hemmer, G. Kasper (Eds.), Institut für Mechanische Verfahrenstechnik und Mechanik der Universität Karlsruhe (TH), Karlsruhe, Glasgow, pp. 185-199.

6. Mai, R., Fronhöfer, M. and Leibold, H. (1996). "Flow Charcteristics of Filter Candles During Recleaning" in "High Temperature Gas Cleaning", Schmidt, Gäng, Pitt, Ditter (eds.), Institut für MUM, Universität Karlsruhe(TH), Karlsruhe, pp.194-206.
7. Stephen, C.M., Grannell, S.K., Seville, J.P.K. (1996), "Conditioning and Pulse-Cleaning of Rigid Ceramic Filters", in "High Temperature Gas Cleaning", E. Schmidt, *et al.* (eds), Institut für Mechanische Verfahrenstechnik und Mechhanik der Universität Karlsruhe (TH), Karlsruhe, pp. 207-218.
8. Grannell, S. K. (1998). "The Industry Application of Low Density Rigid Ceramic Filters for Hot Gas Cleaning". PhD Thesis, University of Birmingham.
9. Kay, J. M. and Nedderman, R. M. (1985). "Fluid Mechanics and Transfer Processes". Cambridge University Press, Cambridge, pp. 544-547.
10. Schiffer, H. P., Renz, U. and Tassicker, O.J. (1989). "Hot Gas Filtration Research at RWTH Aachen PFBC Facilities". Trans. ASME, 1, pp. 487-494.
11. Biffin, M., Panagiotidis, P. and Pitsillides, C. (1997). "Velocity Measurements in a Ceramic Filter Element Undergoing Pulse Cleaning". Proceeding of the Institute of Mechanical Engineers, Part E: Journal of Process Mechanical Engineering, 211, E1, pp.11-16.

Appendix 1

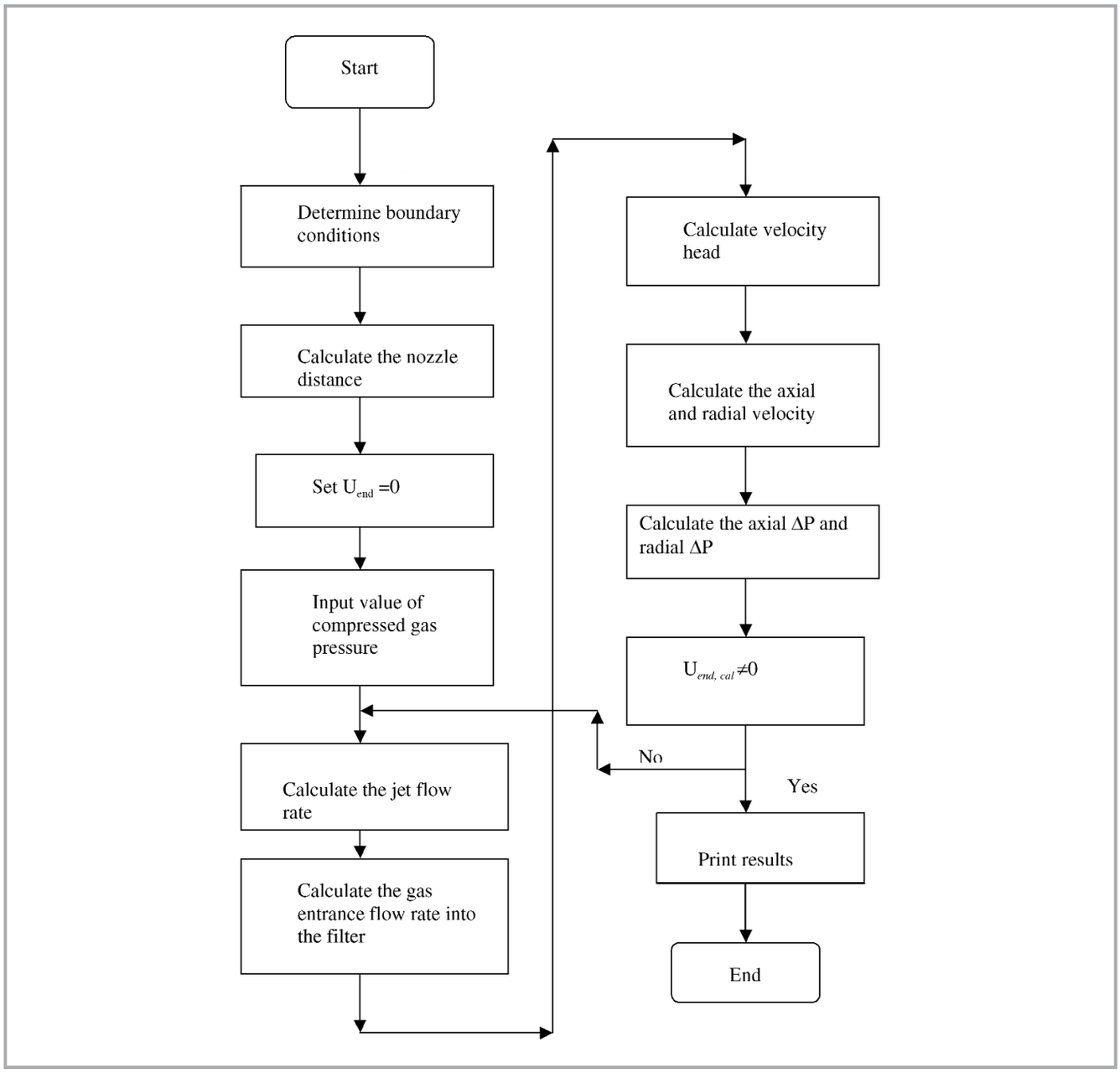

Figure A-1: Flow chart of the model